

3. Surfaces and Interfaces

3-1. Interface Reconstructed Structure of Ag/Si(111) Revealed by X-Ray Diffraction [1]

Investigations of interfaces have technological importance, because the physical properties of semiconductor devices depend on the characteristics of their interfaces. Especially, the effects of reconstructed structures on the preferred orientation of overlayer films have not been fully understood, while control of the crystal orientation of overgrown films is needed in all electric devices from solar cells to superconducting devices.

Recently, interface reconstructions (superstructures) were found in several semiconductor interfaces. The $(\sqrt{3} \times \sqrt{3})$ superstructure (called $\sqrt{3}$ for short) has been reported to exist at the Ag/Si(111)

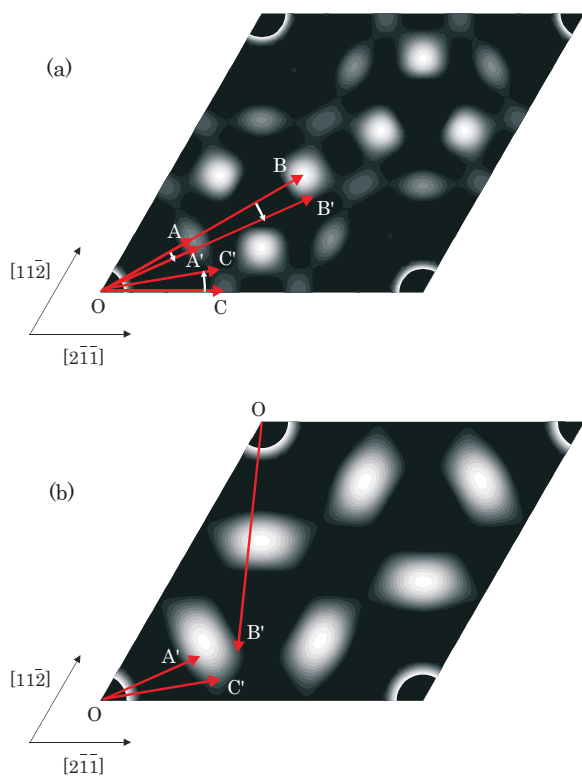


Figure 1. Patterson map of the Si(111) $\sqrt{3}$ -Ag surface structure expected from the HCT model for the Si(111) $\sqrt{3}$ -Ag surface structure (a) and a Patterson map based on the observed structure factors of the Ag/Si(111) $\sqrt{3}$ -Ag interface structure (b).

$\sqrt{3}$ -Ag interface [2]. The interface superstructure is observed when Ag is deposited on a Si(111) $\sqrt{3}$ -Ag surface at a substrate temperature lower than about 300K. We performed grazing-incidence X-ray diffraction experiments at BL-15B2 as a part of an S2-category project (Proposal No. 2000S2-003) and revealed a buried interface reconstructed structure of the Ag/Si(111) $\sqrt{3}$ -Ag in detail.

Figure 1 shows a Patterson map based on the structure factors. Figure 1(a) shows a Patterson map of the Si(111) $\sqrt{3}$ -Ag surface structure expected from a honeycomb chained-triangle (HCT) model [3] for a Si(111) $\sqrt{3}$ -Ag surface structure. In Fig. 1(a), interatomic vectors, as shown in A, B, and C corresponding to the atomic correlation, clearly appear. Figure 1(b) shows a Patterson map based on the observed structure factors of the Ag/Si(111) $\sqrt{3}$ -Ag interface structure. In Fig. 1(b), only broad peaks appear in the Patterson map. This directly shows that the interface structure is different from the Si(111) $\sqrt{3}$ -Ag surface structure.

By evaluating structural models by a reliability factor (R-factor), we found that the $\sqrt{3}$ interface superstructure can be explained by an inequivalent-

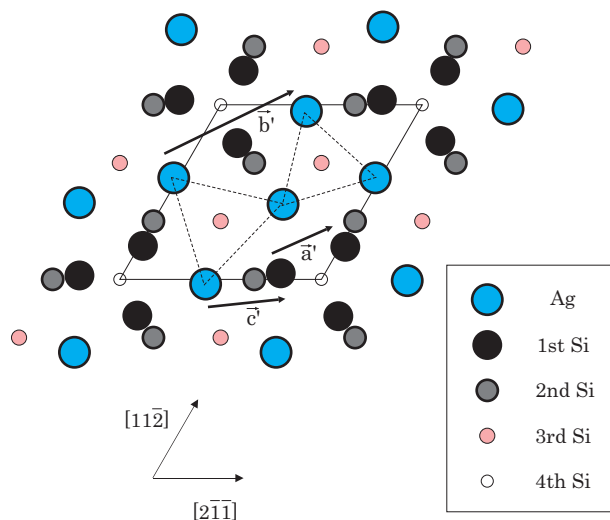
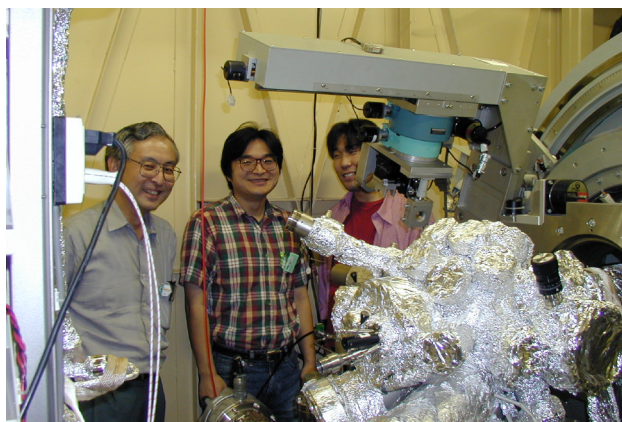


Figure 2. Inequivalent-triangle (IET) model for the Ag/Si(111) $\sqrt{3}$ -Ag interface structure. The atomic correlations (a' , b' , and c') correspond the Patterson peaks (A', B', and C'), as shown in Fig. 1, respectively.



triangle (IET) model [4], as shown in Fig. 2, which has been observed on the Si(111) $\sqrt{3}$ -Ag surface at low substrate temperatures by STM. The calculated structure factors of the IET model were found to be very close to our observed ones. The R-factor using the IET model was less than 25%.

Compared with the HCT model, Ag and 1st-layer Si atoms rotate on the apices of the $\sqrt{3}$ unit cell in the IET model. The rotation angle is about 6 degrees. Thus, the Patterson peaks (A', B', and C') based on the IET model are expected to rotate from the Patterson peaks (A, B, and C) based on the HCT model, as shown in Fig. 1. These Patterson peaks (A', B', and C') correspond to the atomic correlations (a', b', and c'), as shown in Fig. 2, respectively. The superposition of three Patterson peaks (A', B', and C') is thought to give the broad peaks in Fig. 1(b).

In conclusion, by measuring in-plane fractional-order rods we found the in-plane interface structure of Ag/Si(111) $\sqrt{3}$ -Ag to be explained by the IET-model.

K. Akimoto (Nagoya Univ.)

References

- [1] S. Horii, K. Akimoto, S. Ito, T. Emoto, A. Ichimiya, H. Tajiri, W. Yashiro, S. Nakatani, T. Takahashi, H. Sugiyama, X. Zhang and H. Kawata, *Surf. Sci.* in press.
- [2] K. Akimoto, M. Lijadi, S. Ito, and A. Ichimiya, *Surf. Rev. Lett.* 5 (1998) 719.
- [3] T. Takahashi and S. Nakatani, *Surf. Sci.* 282

(1993) 17.

- [4] H. Aizawa, M. Tsukada, N. Sato, and S. Hasegawa, *Surf. Sci.* 429 (1999) L509.

3-2. Initial Oxidation of a Si(111) 7×7 Surface Studied by O K-Edge NEXAFS

Motivated by the importance of thin dielectric layers in the present and future Si device technology, a great deal of effort has been devoted to the study of silicon surface oxidation. Surprisingly, however, a few fundamental issues concerning the adsorption and reaction processes of oxygen molecules on Si surfaces have not been clarified. The major questions under discussion are: (i) whether the dissociation of O₂ involves metastable species or not and (ii) whether the metastable species include any form of molecular species or not.

At present, there seems to be a well-established paradigm that O₂ on a Si(111) 7×7 surface dissociates through a metastable molecular precursor state. However, recently this paradigm, itself, was challenged by an ab initio calculation, which excluded the existence of the molecular precursor on Si(111) and reinterpreted most of the previous spectroscopy and scanning-tunneling microscopy results by metastable and stable atomic adsorbates [1]. This study calls for an urgent and careful reinvestigation of the initial oxygen adsorption on a Si(111) surface. Especially, since the present debate originates mainly from the uncertainty of the experimental probes used to identify the molecular species, a far more molecule-sensitive probe is highly required.

Near-edge X-ray absorption fine structure (NEXAFS) has been established as a powerful tool to obtain information on the local geometry and electronic structures of molecular adsorbates, where the core-level excitations into empty molecular orbitals are detected directly. We applied this technique to the initial oxygen adsorption on a Si(111) 7×7 surface systematically at 30-500 K [2].

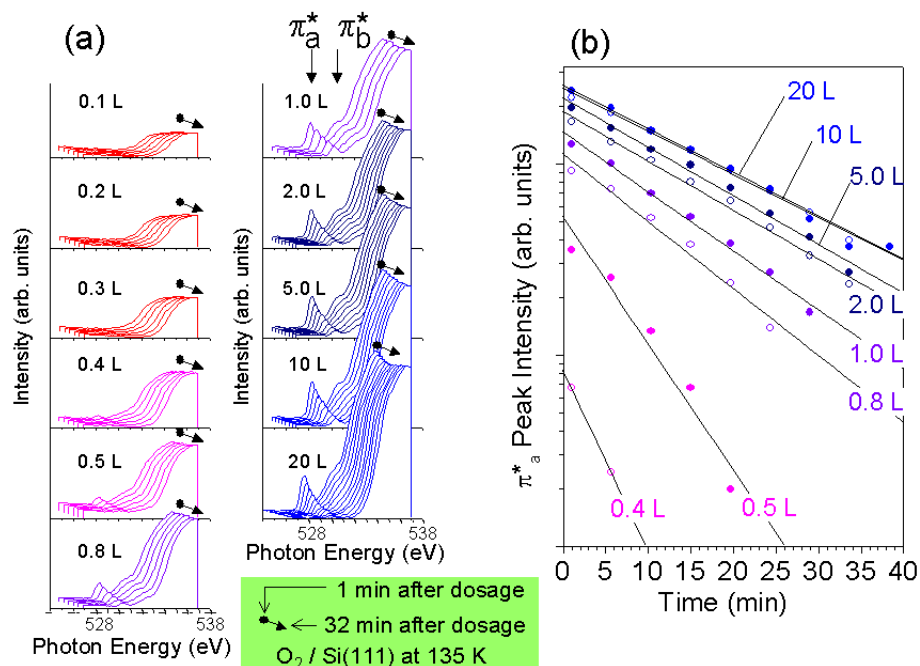


Figure 3.

(a) Series of consecutive O K-edge NEXAFS spectra for the Si(111) 7×7 exposed to O_2 at 135 K. The acquaintance time for one spectrum was 280 s with a time lag between the completion of the O_2 exposure and data acquisition at 530 eV of 60 s (1 L = 10^{-6} torr-s). (b) Time decay of the π_a^* peak intensities for various O_2 dosages at 135 K.

A molecular-adsorption species was identified by distinctive absorption resonances due to the $1\pi_g$ molecular orbitals at temperatures below 220 K (Fig. 3(a)). The molecular species is metastabilized to have a lifetime of 15–35 min. at 135 K. However, a detailed study of the coverage dependence revealed that these molecular species exist only under the presence of atomic adsorbates of more than 0.1 ML (monolayer) (Fig. 3(b)). It is thus clearly evidenced that the very initial adsorption is dissociative, even at 100 K, and the molecular species is not a precursor state.

These molecular species were found to have two distinctive π^* ($1\pi_g$) resonances with a clear polarization dependence. This suggests an on-top adsorption structure of the molecular oxygen possibly with the dissociated oxygen atoms in the back-bond sites stabilizing the molecular adsorbates. The suggested molecular adsorption structures with the coadsorbed oxygen atoms are shown in Fig. 4.

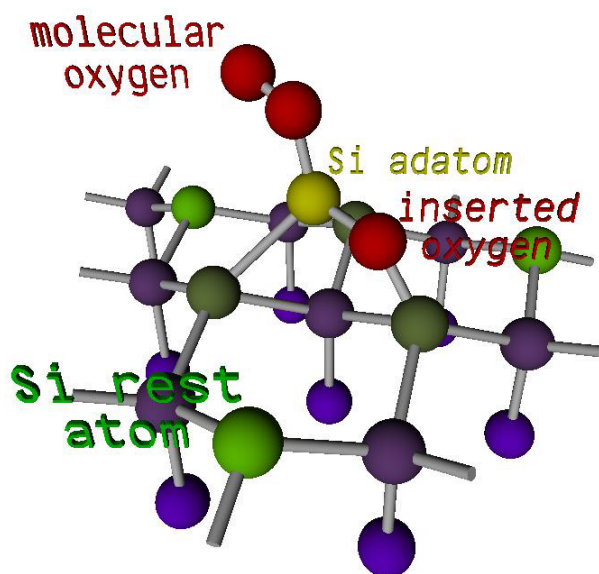


Figure 4.

Structure model for coadsorption of molecular and atomic oxygen adsorbates on Si(111).

F. Matsui¹, H.-W. Yeom², and T. Ohta³ (¹Nara Inst. Sci. Tech., ²Yonsei Univ., ³Univ. of Tokyo)

References

- [1] S.-H. Lee and M.-H. Kang, *Phys. Rev. Lett.* **82** (1999) 968.
- [2] F. Matsui, H.W. Yeom, K. Amemiya, K. Tono and T. Ohta, *Phys. Rev. Lett.* **85** (2000) 630.

3-3. Fermi-Surface Nesting in In/Cu(001)

While exhaustive surface reconstruction takes place on almost all surfaces of covalent semiconductors, very few examples are known for metal surfaces. This is usually ascribed to the nature of metal electrons, which efficiently smear out the potential discontinuity at surfaces without any need to rearrange the atoms. It has also been anticipated that electrons at metal surfaces do not exhibit properties characteristic of low-dimensional systems. We, however, found that the Fermi-surface nesting of the surface-resonance band induces an order–order structural phase transition on the surface of a normal-state metal.

We recently studied the structures and transitions in ultrathin In films on Cu(001) by means of scanning-tunneling microscopy (STM) and low-energy electron diffraction (LEED) [1, 2]. At an In coverage of 0.5, the low-temperature (LT) $(9\sqrt{2}\times 2\sqrt{2})R45^\circ$ phase transformed reversibly to the high-temperature (HT) $(\sqrt{2}\times\sqrt{2})R45^\circ$ ($c(2\times 2)$) phase at 350 K. In order to reveal the mechanism of this phase transition, we studied the valence electronic structure of In/Cu(001) by angle-resolved photoelectron spectroscopy (ARPES) with synchrotron radiation [2]. The experiments were performed at the BL-7B. Figure 5a shows the ARPES spectra taken along $\bar{M}'\text{--}\bar{\Gamma}'_{10}$ for the HT $c(2\times 2)$ phase. An In-induced surface resonance (S_1) is observed at ~ 1 eV in the lowest spectrum corresponding to $\sim 0.4 \bar{M}'\bar{\Gamma}'_{10}$. Note that the S_1 peak is not observed for clean Cu(001). The S_1 peak disperses upward upon approaching $\bar{\Gamma}'_{10}$ and crosses the Fermi level.

We traced the Fermi-level crossing points of the

S_1 band by measuring the ARPES spectra with the emission angle varied in 0.5° interval. Figure 6 shows the Fermi surface determined according to the $c(2\times 2)$ symmetry. The Fermi surface has a square-like shape and defines hole pockets enclosing $\bar{\Gamma}'$ points. The rectangle centered at the $\bar{\Gamma}'_{00}$ represents the SBZ of the LT phase, $(9\sqrt{2}\times 2\sqrt{2})R45^\circ$. Also shown is the Cu bulk Fermi surface projected onto the (001) surface. Note that the projected Fermi surface of bulk Cu is shown for the (1×1) symmetry for comparison purpose, and should actually be rearranged for the $c(2\times 2)$ surface. Therefore, the projected bulk hole pockets around $\bar{\Gamma}'(\bar{M}'$ for (1×1)) disappear for the $c(2\times 2)$ symmetry, which means that the Fermi surface determined for the HT phase is not strictly of 2D nature.

The Fermi wavevector (k_F) along $[100]$ and $[010]$ is 0.30 \AA^{-1} . STM and LEED show that the structure

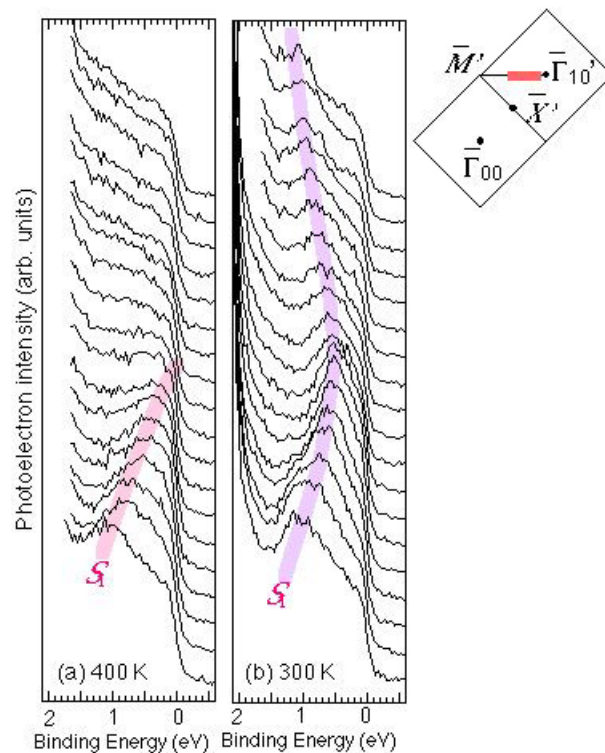


Figure 5. ARPES spectra for In/Cu(001) measured at (a) 400 K and (b) 300 K. The spectra from the bottom to top correspond in reciprocal space to $\sim 0.4 \bar{M}'\bar{\Gamma}'_{10}$ to $\sim 0.9 \bar{M}'\bar{\Gamma}'_{10}$. Photon energy was 22.7 eV.

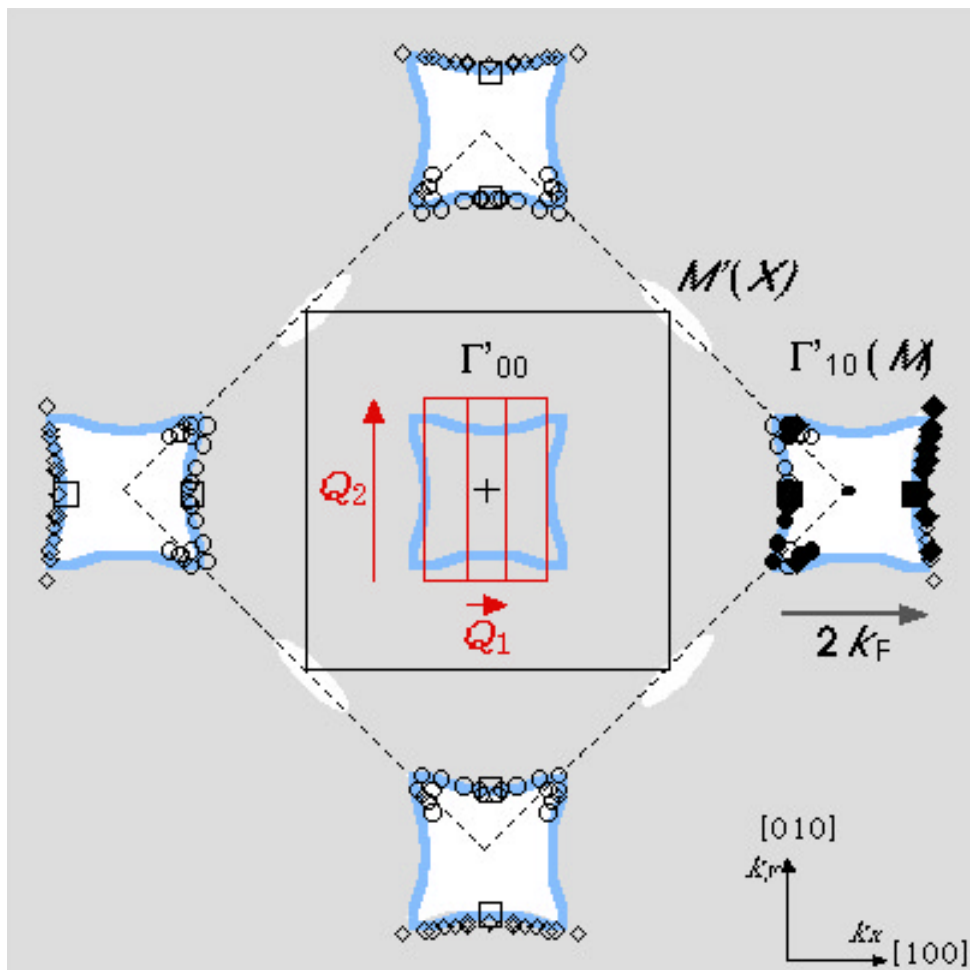


Figure 6.

Fermi surface determined for Cu(001)- c(2x2)-In. The solid symbols indicate actual data points. The open ones were generated by mirror operations, and the gray lines indicate that deduced based on the c(2x2) translational symmetry.

in the LT phase is characterized by the two modulation vectors: $Q_1 = 0.19 \text{ \AA}^{-1}$ along [100] and $Q_2 = 0.87 \text{ \AA}^{-1}$ along [010]. Neither Q_1 nor Q_2 is consistent with a simple nesting condition, $2k_F = Q$. However, as shown in Fig. 6, the Brillouin-zone boundary of the $(9\sqrt{2} \times 2\sqrt{2})R45^\circ$ structure coincides with the Fermi surface of the HT phase. Thus, a 1D generalized nesting condition, $Q_1 = 2k_F/3$, holds for this system.

The Fermi surface nesting manifests itself in the ARPES spectra for the LT phase, as shown in Fig. 5(b). The S_1 band does not cross the Fermi level, but disperses back to higher binding energies beyond $k_x > 1.39 \text{ \AA}^{-1}$, resulting in a large energy gap in

the LT phase. Since energy-gap formation accompanied with partial Fermi surface removal reduces the total energy of valence electrons, the deformation of the lattice in the LT phase is stabilized.

T. Aruga (Kyoto Univ.)

References

- [1] T. Nakagawa, S. Mitsushima, H. Okuyama, M. Nishijima, and T. Aruga, to be published.
- [2] T. Nakagawa, G.I. Boishin, H. Fujioka, H. W. Yeom, I. Matsuda, N. Takagi, M. Nishijima, and T. Aruga, Phys. Rev. Lett. 86 (2001) 854.